Processing-induced morphology: Its relationship with tensile impact behaviour in injection-moulded polypropylene

Eric Lafranche, Grégory Brassart, Patricia Krawczak

Processing-Induced Morphology: Its Relationship with Tensile-Impact Behaviour in Injection-Moulded Polypropylene

Eric LaFranche*, Grégory Brassart and Patricia Krawczak
Ecole des Mines de Douai, Polymers and Composites Technology Department, 941 rue Charles Bourseul - BP 10838 – 59508 Douai Cedex - France

This paper aims at identifying the main parameters that govern the tensile-impact strength of injection-moulded polypropylene. A Taguchi Design of Experiments (DOE) analysis has shown that the key parameters in both flow and transverse directions are the polymer melt and mould temperatures and the volumetric flow rate. The differences in high-speed mechanical behaviour have been explained on the basis of an investigation of the processing-induced morphology/tensile-impact behaviour relationship. The microstructure of parts manufactured under two extreme sets of moulding conditions has been analysed through-the-thickness by means of microscopy observations and by measurements of crystallinity, molecular orientation and thermal expansion. The impact brittleness originates from the skin layers, the major influential parameters being the skin/core ratio and the crystalline structure. The crack initiation energy increases with the oriented skin layer thickness, whereas the brittleness increases with the crystallinity level and the spherulite size.

INTRODUCTION

During high volume manufacturing of automotive polypropylene parts by injection moulding, some scattering is frequently observed in the mechanical properties, and especially the impact properties. The brittle fracture obtained under impact loading is suspected of depending significantly on the processing parameters and their fluctuations.

Two basic deformation mechanisms (shear deformation and deformation due to crazing/voiding) are observed for all thermoplastic materials. The first occurs at a more or less constant volume and is associated with ductile behaviour[1]. The second is related to cavitation and is associated with brittle behaviour, as it involves both a local plastic deformation and the first step of the fracture process[2]. Each mechanism has its own induction or relaxation time. The above-mentioned crazes result from a plastic deformation process, which induces micro-voids in the polymer. These crazes have a trans-spherulitic growth. Because of competition between these two plastic deformation mechanisms, crazing/voiding and shearing associated with plastic yielding, the thermoplastic's mechanical behaviour is characterized by a brittle–ductile transition or a brittleness temperature[3]. Both craze/void creation and shear deformation are thermally activated phenomena, which depend also on parameters such as loading rate and polymer structure. The brittleness temperature shifts towards higher temperatures in the case of a loading rate increase. Also, for semi-crystalline materials such as polypropylene, an increase in the crystallinity level increases the yield strength, the brittleness temperature and therefore the brittleness[4,5].

Regarding the relationship between morphology and the impact fracture behaviour of polypropylene, Karger-Kocsis[6] has shown that the plastic deformation decreases when the spherulite diameter increases due to micro-void formation and a low concentration of "link chains" at the inter-spherulitic frontiers. The micro-cracks and inter-spherulitic fractures are predominant[7,8]. Varga[9] explains that the above-mentioned frontiers are

*lafranche@ensm-douai.fr

weak zones where micro-voids favour the initiation and propagation of cracks. Moreover, Ouederni and Philips[10] have pointed out that for a given spherulite size, the higher the crystallinity level is, the lower the fracture resistance and the higher the crack propagation velocity. They have also shown that nucleation agents contribute to a slightly delayed crack initiation and to an increase in the crack propagation velocity.

In the case of injection-moulded parts, the molecular orientations due to the melt flow and the cooling rate through-the-thickness induce morphological gradients. This involves a non-homogeneous structure that can be compared to a laminated composite where each elementary layer brings its contribution and influences the mechanical behaviour of the parts[11]. Many authors[12-14] have studied these skin-core structures. Three main zones can be usually distinguished in injection-moulded parts. The first is a skin zone at the mould wall with a high level of molecular orientation parallel to the injection direction, but no distinguishable crystalline morphology at the optical microscopy observation scale. The second zone, characterised by an oriented row structure and named the shear zone, has a spherulitic morphology (most of the spherulites consist of hexagonal β phases), where the lamellae are oriented perpendicularly to the surface (but less and less oriented in the flow direction). Further investigations have led to a more accurate description of the shear zone that divides it into three parts (fine spherulitic structure; texture showing preferred orientation, and fibrous transcrystalline structure). The last zone is a spherulitic core of α–monoclinic phases with no preferred orientation[13]. More recently, Varga *et al.*[15] have considered β nucleated polypropylene and have distinguished three sub-layers in the skin (from the surface towards the core): a transcrystalline zone at the mould interface, a spherulitic zone and a cylindritic layer caused by melt shearing. The thickness of each zone, the crystal shapes and the orientation level are influenced by the processing conditions[12,14,16,17]. Their relationships with the impact strength have been studied in special cases. For example on the basis of multi-axial impact tests, Cunha *et al.*[18] have shown that the crack initiates in the skin layer zone because of the sample deflection induced during the first step of the impact loading. These authors noticed an impact strength increase with skin layer thickness. Fujiyama[19] *et al.* explained that the planar molecular orientation of the skin governs the part's brittleness. Thus the ductility increases with the orientation level of the skin.

This present paper aims at contributing to an understanding of how the local microstructure (characterized by the molecular orientation gradients through the thickness and the morphological gradient) affects the impact behaviour of injected polypropylene parts. We focus on the relationship between the skin-core effect and (i) the high-speed loading behaviour (ii) the structure-related brittleness.

EXPERIMENTAL

Material

The material studied was a homopolymer polypropylene (Hostalen PPU X9057 HS, Targor) with a Melt Flow Index (MFI) of 11 g/10 min (ISO 1133).

Machine and Mould

The injection moulding machine used (DK Codim) had a 2000 kN clamping force, a gate in the parting line and a standard 42 mm diameter screw. The moulded part was a rectangular 150 mm x 100 mm x 2 mm plate fed by a 2 mm thick fan gate across the entire width. The thermal regulation of the mould was made by means of independent channels, which ensured that the surface temperature was homogeneous to an accuracy of ±1 °C.

Processing Conditions

A Design Of Experiments (DOE) analysis was devised in order to understand the effects of processing conditions on the impact properties. The Taguchi L16 (2^{15}) table used included six parameters related to the filling, holding and plasticisation stages (Table 1) and six interactions between parameters, as shown in the linear graph

Table 1. Processing conditions for Taguchi DOE

Parameters	Symbol	Low Limit	High Limit
Mould Temperature (°C)	MoT	25	75
Melt Temperature (°C)	MeT	230	270
Volumetric flow rate (cm^3/s)	IS	55	138
Holding Pressure (Bar)*	HP	30	65
Back Pressure (Bar)*	BP	8	14
Screw rotation speed (min^{-1})	SRS	100	150
**(1 Bar = 10^5 Pa)*			

Figure 1. Linear graph for Taguchi DOE

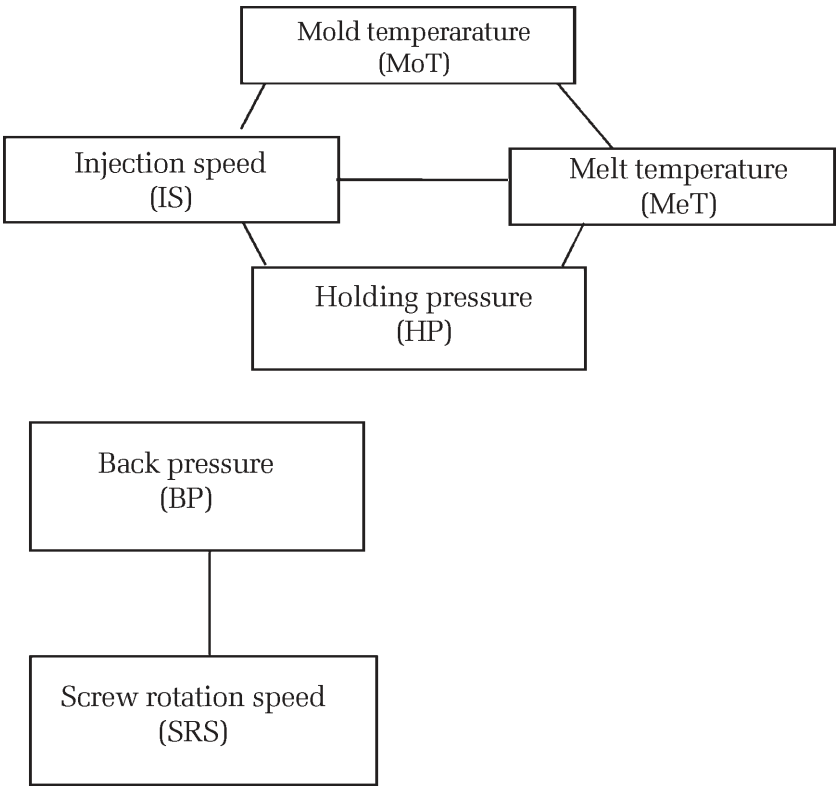

(Figure 1). The level of each factor was determined from the polypropylene supplier's data sheet. The other processing parameters (holding time, packing pressure, cooling time etc) were kept constant.

Mechanical Testing

The output parameter of the Taguchi DOE was the part's tensile-impact strength. Sets of five ISO ½ test samples were tested according to ISO 8256 on a pendulum tensile-impact machine (Zwick). A 1.010 kg impactor was used. The impact velocity was 3.85 m/s. The tests were carried out in both flow (longitudinal) and transverse directions (see the cutting pattern in Figure 2). The sample was clamped between the mobile grip and the fixed grip of the tensile impact tool (Figure 3). When the pendulum reached its lowest point, it hit the mobile grip and the tensile load was transmitted to the sample.

The tensile impact behaviour law was also recorded on sets of 10 longitudinal test samples using a high-speed tensile machine at a displacement rate of 2 m/s (Lhomargy) with a 30 mm clamping jaw distance (Figure 4). The data acquisition frequency was set

Figure 2. Test sample cutting pattern

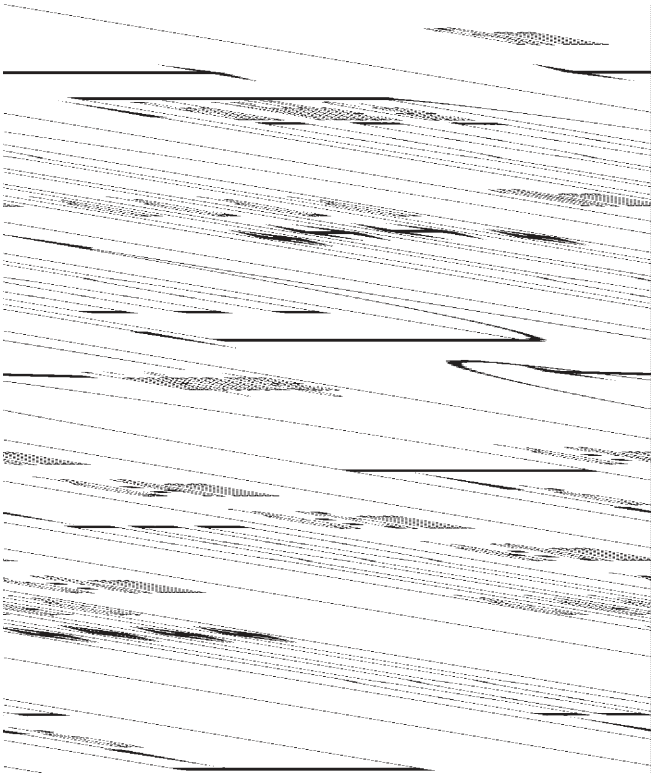

Figure 3. Principle of the pendulum tensile-impact machine

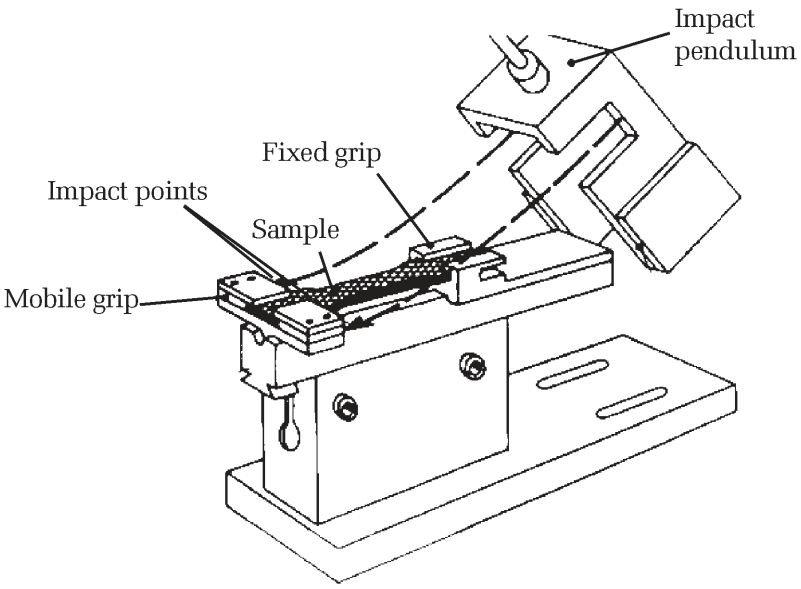

Figure 4. Principle of the high-speed tensile machine (F = Force, D = Displacement, t = time)

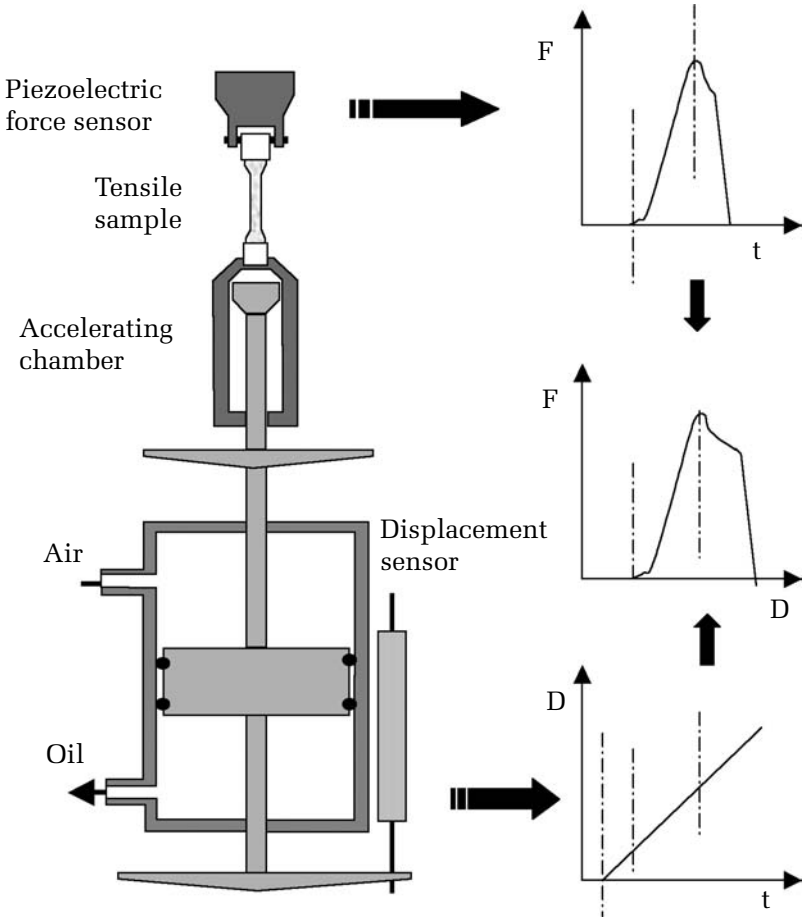

at 10 MHz. The maximum force, yield strength, elongation, crack initiation, crack growth and total energies were determined from the recorded force versus displacement curves.

Molecular Orientation Measurement

Molecular orientation was measured by the infrared dichroïsm method on microtome slices (10 mm x 6 mm x 20 µm) cut through the thickness of the moulded plates. The measurement leads to the calculation of the second moment of the global orientation function or orientation factor[20,21]. This allows separating orientations for both crystalline and amorphous phases of the polymer. The second order moment of the orientation function, known as Herman's orientation function, is given by Equation 1:

$$f = \langle P2\cos\theta \rangle = \frac{3\langle \cos^2\theta \rangle - 1}{2} \qquad (1)$$

where θ is the angle between the chain axis and a chosen reference axis (usually the flow direction). When the polymer chains are aligned along the reference axis, i.e. θ = 0° for all chains, f = +1, whereas in the case of perpendicular orientation, i.e. θ = 90°, f = -0.5. For a random orientation it can be shown that f = 0.

The absorption bands used were those usually chosen for polypropylene[22] (973 cm^{-1} and 998 cm^{-1} for the pure amorphous and crystalline phases respectively). FT-IR spectra were obtained from a Fourier Transform Infrared spectrophotometer (Perkin Elmer). The microtome slices were fixed on a sample holder with a polarizer. The absorbance measurements were made for each IR absorption band with polarisations parallel and perpendicular to the flow direction. In this study, only the crystalline absorption band was considered.

Thermal Expansion Measurement

The thermal expansion was measured on microtome slices (2 mm x 0.5 mm x 20 µm), according to a method developed by Delbarre[22] (Figure 5). The thin slices were peeled off from larger samples (10 mm x 6 mm) cut along the flow axis. The slice was then placed between two cover glasses on a heating stage located under a microscope used in transmission mode (Jenapol). A CCD camera transmitted the image to a computer equipped with image processing software (Visilog 5.2, Noesis).

Figure 5. Measurement apparatus for determining thermal stresses by Dilatometric Analysis of Image (DAI)

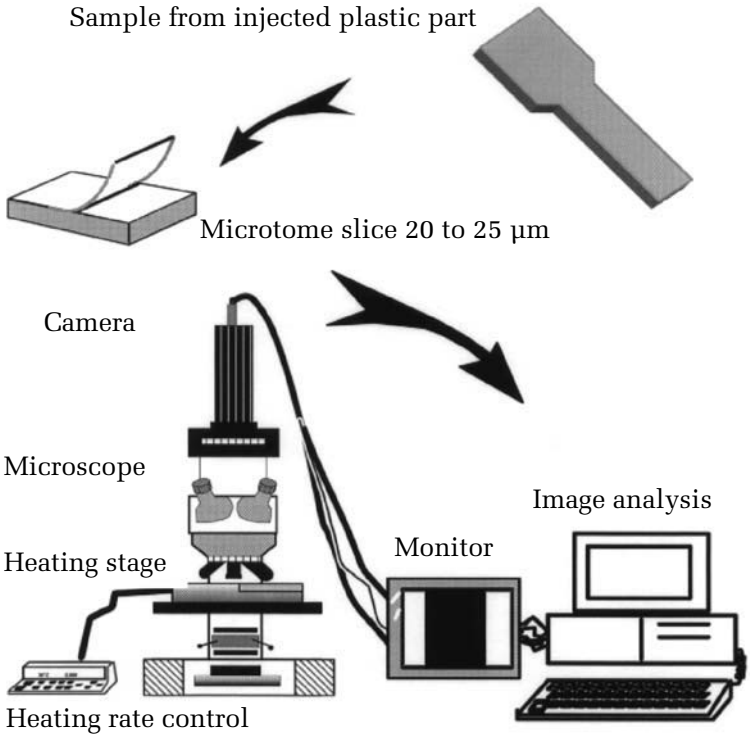

The processing was achieved on images of 512 x 512 pixels. The sensitivity was about 1 pixel, leading to an accuracy of 0.02% for the strain calculation. The heating rate was 5 °C/min.

The slice thermal expansion was recorded versus temperature for two successive thermal treatments between 30 °C and 100 °C. During the first treatment, the total strain was a reflection of the addition of pure thermal expansion and the relaxation of thermally induced internal stresses. During the second treatment, only pure thermal expansion occurred (Figure 6).

Crystallinity Measurement

The degree of crystallinity was measured on a differential scanning calorimeter (DSC, Perkin Elmer) with a heating rate of 20 °C/min. From the melt enthalpy ΔH (Equation 2), the degree of crystallinity X_c was calculated using the melt enthalpy of a 100% crystalline polypropylene ΔH_0 (Equation 3):

$$\Delta H = K \frac{A}{m} \qquad (2)$$

$$X_c = 100 \cdot \frac{\Delta H}{\Delta H_0} \qquad (3)$$

where A = peak area

ΔH = melt enthalpy of PP

ΔH_0 = melt enthalpy of a 100% crystalline PP (148 J/g)

m = sample weight

K = apparatus constant

The measurements were carried out three times per sample on the plate symmetry axis.

Microstructure Analysis

A qualitative assessment of the injection-moulded part's microstructure was carried out through-the-thickness by polarized optical microscopy (Jenapol) of 20 µm thick microtome slices peeled in the part's centre. The crossing angle of the polarizer and the analyser was 0-90°. A λ monochromatic filter placed between them and the thin slice had a 45° inclination angle so as to obtain the maximum birefringence intensity.

PROCESSING CONDITIONS / IMPACT STRENGTH RELATIONSHIP

Table 2 summarizes the tensile-impact strength results obtained from the DOE. The impact strength variation between the minimum and maximum values (about 45% in the longitudinal (flow)

Figure 6. Typical curves obtained by DAI

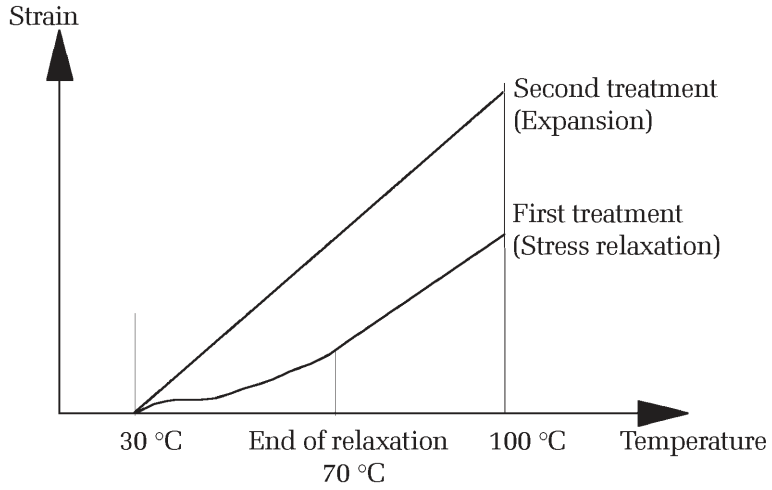

direction and more than 30% in the transverse direction for the three sample locations) indicated the significant influence of the processing conditions. An increase in the impact strength along the flow axis could also be noticed in the transverse direction (Figure 7), showing the effects of flow length and micromorphology variations.

The influence of the different processing parameters (and of their interactions) on the impact strength measured in both the longitudinal (flow) and transverse directions is reported in Figure 8. On this basis, it was possible to distinguish the factors and interactions that were very significant (relative contribution higher than 15%) from those that were less important (contribution between 10 and 15%) or even negligible (contribution lower than 5%).

Analysis in the Flow Direction

The volumetric flow rate (IS) was the only significant factor in the flow (longitudinal) direction. The effects of the other factors on the tensile-impact strength were globally negligible, as shown in Figure 8. Moreover, the interaction between the mould temperature and the volumetric flow rate (MoT-IS) was preponderant and highly significant; those between the polymer melt temperature and the volumetric flow rate (MeT-IS) or the holding pressure (MeT-HP) cannot be neglected. The maximum

Table 2. Tensile-impact strength values from the DOE

			Tensile-impact strength kJ/m² (*)		
			Minimum	**Maximum**	**Average**
Sample location	**Longitudinal**		575 *(25)*	841 *(21)*	691 *(71)*
	Transverse	Gate	469 *(25)*	602 *(26)*	531 *(44)*
		Middle	473 *(21)*	631 *(42)*	545 *(49)*
		End	497 *(26)*	657 *(36)*	584 *(44)*

** (Values in brackets are standard deviations)*

Figure 7. Influence of flow length on the tensile-impact strength in the transverse direction

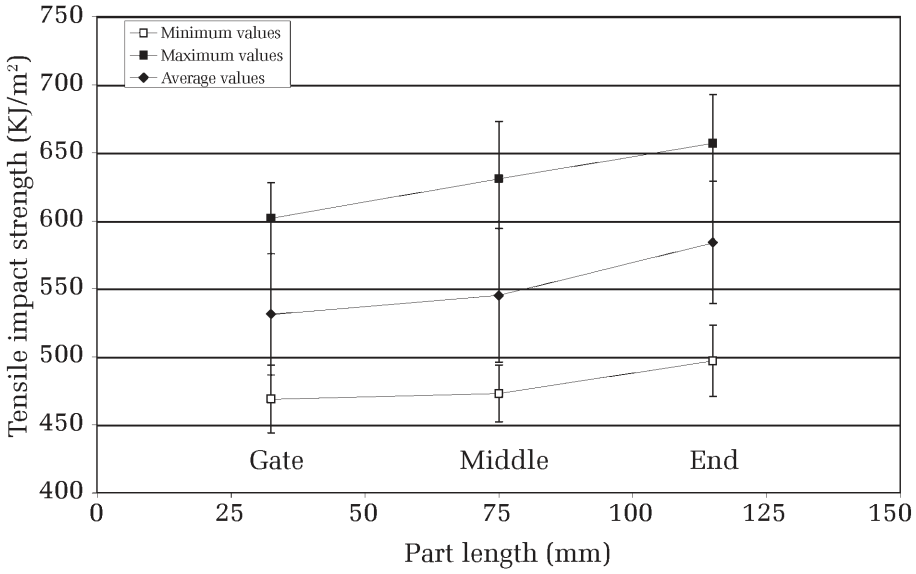

Figure 8. Influence of processing parameters on the tensile-impact strength, from the DOE analysis

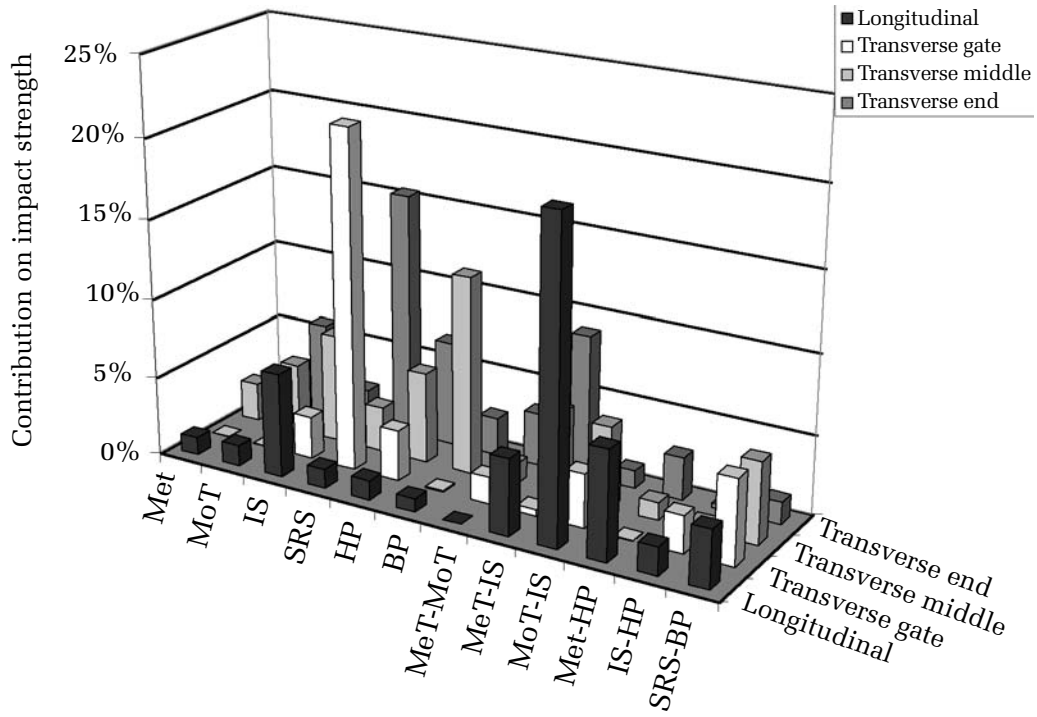

Figure 9. Effects of processing parameters on the longitudinal tensile-impact strength (standard deviations represents data scattering when the considered factor is set up at its low (1) or high (2) level in the Taguchi DOE)

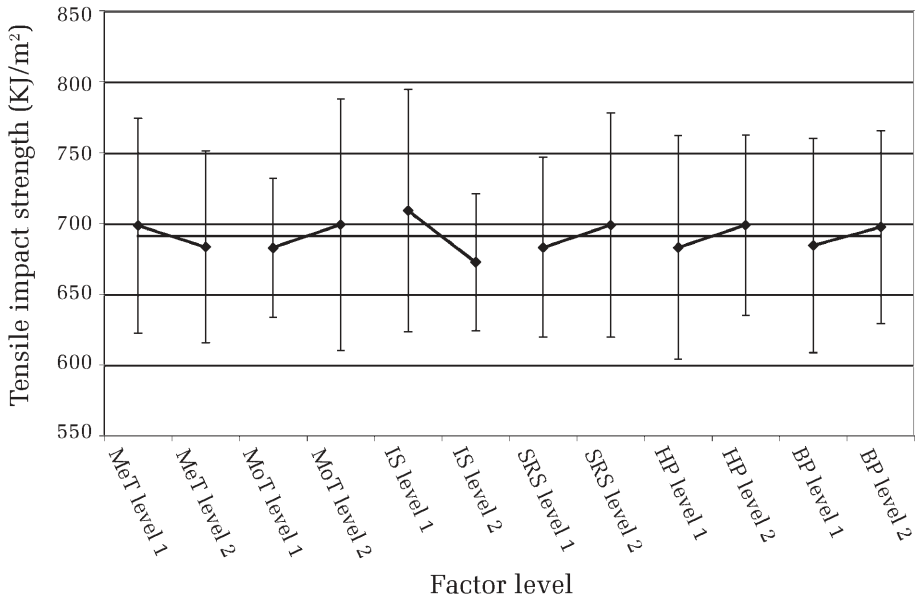

tensile-impact strength in the flow direction was obtained using low polymer melt temperature and volumetric flow rate, and high mould temperature, screw rotation speed, holding pressure and back pressure (Figure 9).

Such trends were expected because low levels of polymer melt temperature and volumetric flow rate favour shear flow within the melt during the filling stage. This increases the thickness of the oriented layers and improves the impact strength, as already

noticed by other authors[18,23]. Furthermore, polymer melt and mould temperatures as well as holding pressure are parameters that govern the relaxation of the molecular orientation induced during mould filling, and thus the skin thickness and the crystalline morphology of the part. Their effect on impact strength is therefore logical.

Analysis in the Transverse Direction

In the transverse direction, Figure8 shows the importance of some indirect effects of temperature (mould or polymer melt temperature) with screw rotation speed and back pressure. The holding pressure was also a significant factor. Its influence was greater at a location far from the gate; the higher transverse tensile impact strength was obtained far from the gate (Figure 7) and when the holding pressure was set at a low level. This is due to the fact that a high holding pressure induces flow movements and therefore extra molecular orientation in the flow direction. Consequently orientations and mechanical properties were lower in the transverse direction. This effect was greater near the gate.

DISCUSSION

The Taguchi DOE analysis has shown that the main factors acting on the tensile-impact strength are essentially the molecular orientations induced by the volumetric flow rate and the crystalline morphology, linked to the cooling rate.

Through-the-Thickness Microstructural Analysis

Therefore the microstructure of each part moulded under different processing conditions (Taguchi DOE) was qualitatively evaluated through-the-thickness (a relatively coarse analysis). As previously observed by other authors[12,24], each slice peeled in the centre of the plate (Figure 10) had a multilayered structure, with five main layers through the thickness (Figure 11):

- 2 highly oriented skin layers (the lighter zones, I and Ib)
- 2 intermediate layers (II and IIb)
- 1 non-oriented core layer (the dark zone, III)

Table 3 summarizes the results (the thickness of each layer, and the impact strength) obtained for each of the 16 sets of processing parameters. The part's structure dependence on the processing parameters clearly appears. It is interesting to focus on tests N° 5 and N° 9, which lead to the maximum and minimum tensile-impact strength values respectively. In both cases the oriented layer thickness was above the

Figure 10. Slice location in the part for optical microscopy analysis

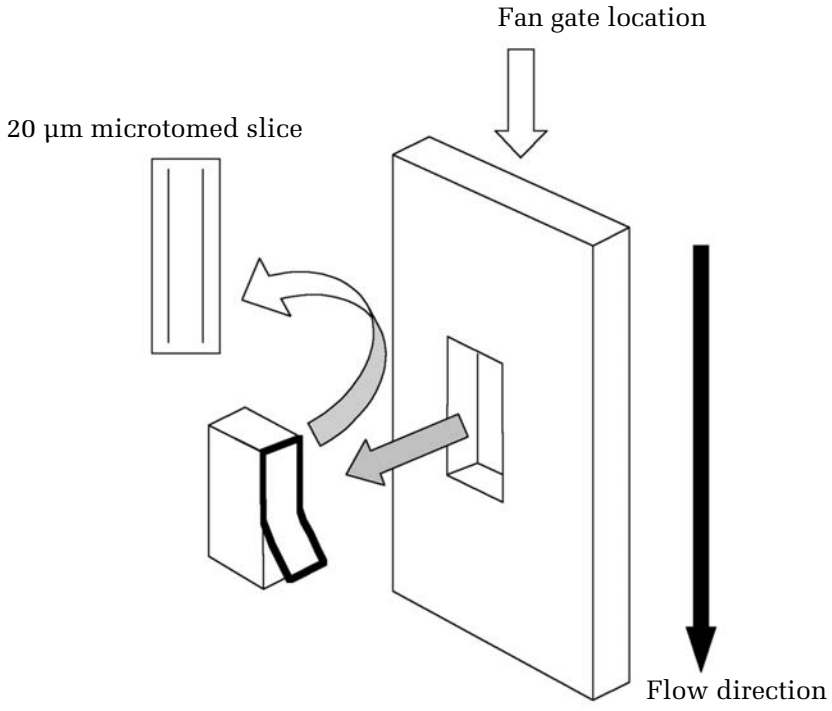

Figure 11. Through-the-thickness multilayer structure of the microtome slices

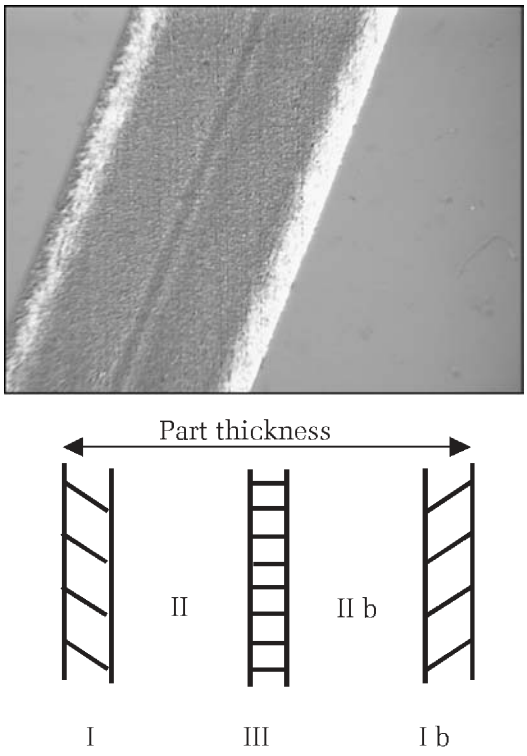

average. Thus it was worth carrying out an in-depth analysis for these two opposite moulding conditions (Table 4) to explain the large difference in the tensile-impact strength values. Processing parameter sets N° 5 and N° 9 were actually characterized by opposite extremes of mould and polymer melt temperature. Condition N° 5 corresponded to a low melt temperature and a high mould temperature (and inversely for condition N° 9).

The first step in the analysis aimed at evaluating the effective incidence of the two skin layers (I and Ib) on the impact properties. Test samples were therefore peeled on their two faces in order to remove the skin layers and then tested again. The results reported in Table 5 show the great influence of these skin layers on the tensile-impact strength. The origin of such large differences can be explained by considering the two major factors (% crystallinity and molecular orientation in the testing direction) that influence the tensile-impact mechanical behaviour of an injection-moulded part.

Crystallinity

Processing parameters sets N° 5 (low melt temperature and a high mould temperature) and N° 9

Table 3. Layer thickness and longitudinal tensile-impact strength as a function of processing parameters (from Taguchi DOE)

DOE Test	Thickness of the layers in the microtome slices (µm)					Impact strength
N°	I	II	III	II b	I b	kJ/m²
1	183	-	-	-	183	684
2	182	806	115	836	180	673
3	179	830	180	750	153	724
4	184	858	111	812	195	681
5	293	668	79	652	297	841
6	305	710	131	615	352	755
7	79	853	116	864	89	616
8	257	743	101	729	254	609
9	215	727	152	704	192	575
10	138	860	122	845	134	691
11	131	803	200	765	132	688
12	105	847	148	852	130	741
13	234	660	143	721	228	650
14	195	710	326	685	200	800
15	115	790	175	881	45	682
16	180	705	378	715	153	636

Table 4. Processing conditions relating to the maximum (N° 5) and minimum (N° 9) tensile-impact strength results

Processing parameters	Symbol	Test N° 5	Test N° 9
Mould Temperature (°C)	MoT	75	25
Melt Temperature (°C)	MeT	230	270
Volumetric flow rate (cm^3/s)	IS	55	55
Holding Pressure (Bar)*	HP	30	30
Back Pressure (Bar)*	BP	14	8
Screw rotation speed (min^{-1})	SRS	150	150
**(1 Bar = 10^5 Pa)*			

Table 5. Influence of the skin layers on the tensile-impact strength

Processing parameters set N° (Taguchi DOE)		Tensile-impact strength (kJ/m²)	
		Test 5	Test 9
Without skin layers	Single values	583	554
		556	559
		616	555
		601	553
	Average	**589**	**555**
With skin layers		**841**	**575**

(high melt temperature and a low mould temperature) respectively induced degrees of crystallinity of 51% and 61% for tests N° 5 and 9. This may already partly explain the higher brittleness noticed in the samples moulded under N° 5 conditions, as mentioned by other authors[1,2,3,8,23].

Molecular Orientation

Furthermore, it was also interesting to quantify the effective molecular orientation state through the thickness by infrared dichroism. This analysis led to a finer assessment of the structure developed during each step of the injection process, as described elsewhere[11,22,26,27]. Therefore the "skin layer" previously designated by I (Figure 11) can be divided into two sub-layers (designated by 1 and 2; Figure 12). The orientation levels for both opposite processing conditions sets were low (Figures 12 and 13). There was no preferential orientation in the flow direction (<P2cos θ> below 0.7). The orientation profiles were nevertheless similar to those observed by other authors, with four characteristic zones (and thus seven layers)[11,26,28]. The zones were as follows:

A first zone **(1)** where orientation increased due to shear stresses and fountain flow during the

Figure 12. Molecular orientation and thermal expansion versus thickness for sample N° 9

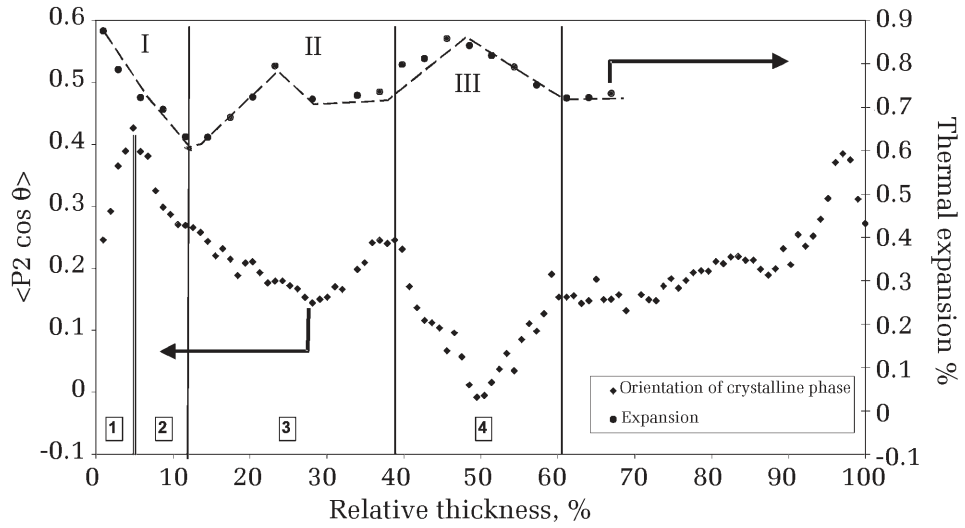

Figure 13. Molecular orientation and thermal expansion versus thickness for sample N° 5

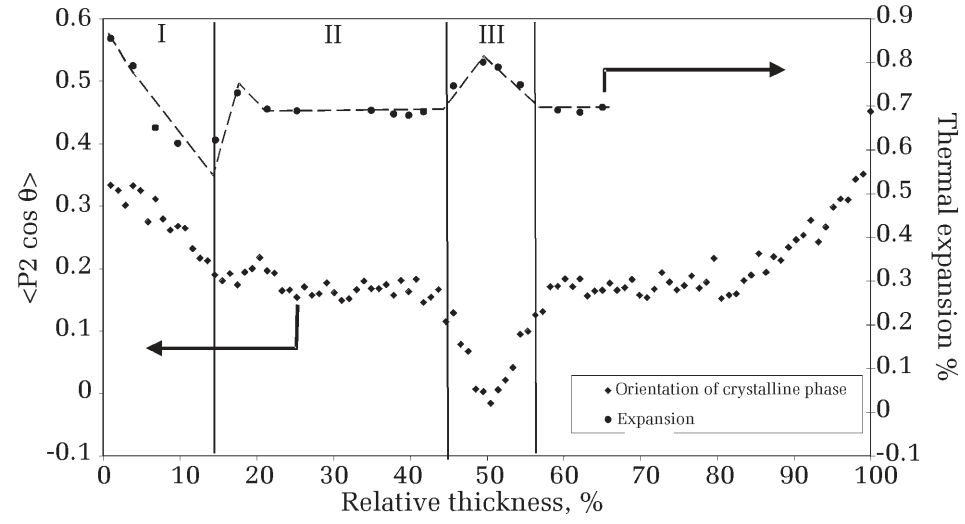

filling stage of the cavity (about 5% of the total thickness).

A second zone **(2)** where orientation decreased rapidly. This was attributed to the quenching effect of the packing pressure that displaces the crystallization isotherm towards the centre of the part[12,29].

A third zone **(3)** where the orientation was due to the holding pressure[28].

A fourth zone **(4)** where the relaxation was preponderant, leading to an isotropic polymer[13].

Sample N° 9 had a higher molecular orientation in the shear zone that confirmed a fast orientation freezing near the wall, because of the low mould temperature (Figure 12). After mould filling, the molecular relaxation effect was significant and the holding pressure lost its efficiency. In the case of the higher mould temperature (sample N° 5), the relaxation effect acted in the shear zone but the holding pressure efficiency limited molecular relaxation during part cooling, leading to a 15% thick oriented zone near the wall (Figure 13).

Thermal Expansion

The structural organisation resulting from molecular orientations and crystalline morphology was also highlighted on thermal expansion profiles after relaxation of the thermally induced internal stresses (Figures 12 and 13). This analysis technique is however less accurate than the molecular orientation measurement and leads to a coarser analysis. Therefore, only three main zones (and thus five layers) could be distinguished in this way. A minimum thermal expansion was noticed just under the skin layer (frontier **I/II)**, which was representative of a well organised structure. The expansion increased in the core layer **(III)** where the polymer was isotropic. These three zones correspond to those already observed by optical microscopy (Figure 11).

The thickness of the central isotropic layers **(III)** observed for samples N° 5 and N° 9 were in accordance with the molecular orientation profiles, showing a thicker layer for the moulding conditions N° 9. The minimum thermal expansion was measured just under the oriented skin layers **(I/II)**. This oriented crystalline area was almost 5% thicker for sample N° 5 than for sample N° 9. In the intermediate shear zone **(II)** the thermal expansion of sample 5 (0.67%) was slightly lower, revealing a more oriented crystalline structure than that of sample 9 (0.72%).

Structure / Impact Behaviour Relationship

The above analysis is in accordance with the tensile impact strength results with and without skin layers (Table 5, Figure 3). Considering molecular orientation, the more oriented skin layers resulting from moulding conditions N° 5 contributed to the higher tensile-impact strength. Considering the morphology, the more crystallized but less oriented layers of sample N° 9, explain the brittleness observed for these moulding conditions because crystalline growth is favoured by a high melt temperature. It is thus possible to assume that a large spherulite size and a poor concentration of "link chains" explain the decrease in tensile-impact strength[25,27]. In contrast, the higher viscosity resulting from the lower melt temperature of moulding condition N° 5 should favour small spherulite size and a high concentration of "link chains". Combined with the orientation profile, this effect tends to increase the tensile-impact strength.

Finally, the force-displacement curves recorded during instrumented high-speed tensile tests (Figures 4 and 14) enabled us to separate the level of significance of different factors (force, strain etc) for the tensile-impact strength. Stress oscillation could be noticed from the records. The stress oscillation due to dynamic tensile impact is an experiment-related artefact that appears in many thermoplastic polymers [30]. The yield strengths were similar for both tests N° 5 and N° 9 (Table 6). However, the crack initiation and crack growth energies respectively were 13% and 45% higher in the case of test sample 5 (Figure 14). As for pendulum tensile-impact tests, they indicated that the tensile strength of the oriented skins was higher than that of the core. However, it was the microstructure (spherulite diameter and crystallinity level) that controlled the energy dissipation capacity and thus the fracture growth phase.

CONCLUSIONS

The main processing parameters that strongly influence the tensile-impact properties and the brittleness of injection-moulded polypropylene parts (essentially polymer melt and mould temperature, and volumetric flow rate) have been experimentally

Figure 14. Typical high-speed tensile behaviour for samples N° 5 and N° 9

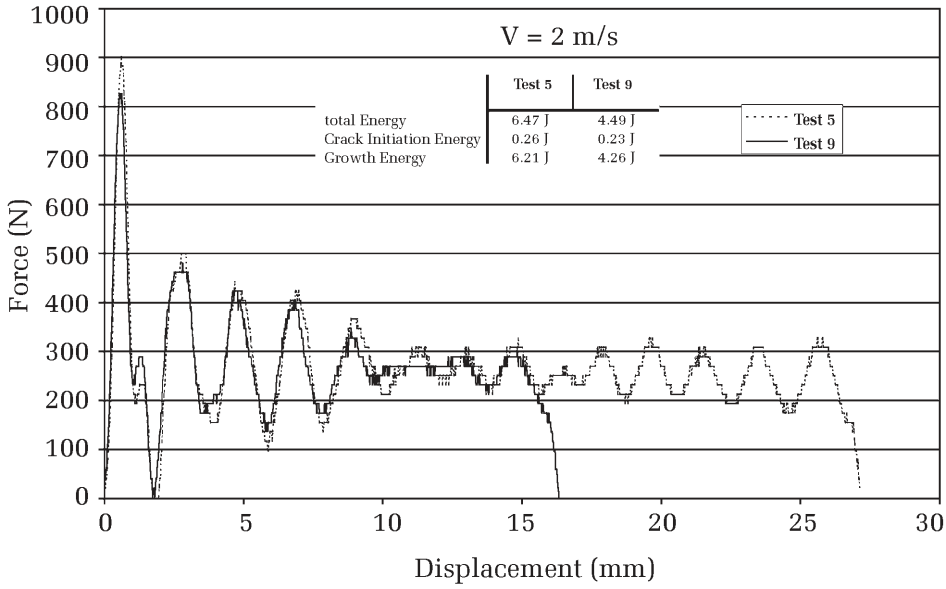

Table 6. High-speed tensile test results			
Processing parameter set N° (Taguchi DOE)	**Units**	**Test N°5 (*)**	**Test N°9 (*)**
Maximum force	N	948 *(99)*	903 *(79)*
Yield strength	MPa	100 *(10)*	94 *(8)*
Elongation	%	59 *(10)*	36 *(7)*
Tensile-impact strength	kJ/m^2	774 *(107)*	469 *(76)*
** (Values in brackets are standard deviations)*			

identified. The differences in mechanical behaviour observed during high volume manufacturing have been explained on the basis of an investigation of the processing-induced morphology/tensile-impact behaviour relationship. Microscopy observations, crystallinity level, molecular orientation and thermal expansion measurements through-the-thickness of injection-moulded parts have led in particular to the following conclusions:

- The brittleness of the injection-moulding part depends on the skin layer's morphology and the skin/core ratio.
- The skin/core ratio depends significantly on the processing parameter setting for each injection moulding phase (filling, packing, holding and cooling stages), which acts directly on the crystallinity level and the spherulite size, as well as on the molecular orientation.
- The tensile-impact strength of the injection-moulded parts is governed by the oriented layer thickness, which is related to both melt flow and cooling rate, directed by processing conditions.
- The energy absorption before crack initiation is influenced more by the thickness of the oriented skin layers than by their molecular orientation (in the case of a limited increase in molecular orientation).
- The crack initiation and crack growth are directly related to the polymer's crystalline structure, in particular the spherulite size, and thus to the concentration of "link chains".

ACKNOWLEDGMENT

Thanks are due to FAURECIA Research Directorate for the financial and technical support and to the European Union (FEDER, European Funds for Regional Development) for contributing to funding the equipment.

REFERENCES

1. **Bucknall, C.B.**, Toughened Plastics, Materials Science Series, Applied Science Publishers Ltd., London, (1977).

2. **Bucknall, C.B.**, Advances in Polymer Science, 27, (1978), 121-148.

3. **Tancrez, J.P.**, PhD Thesis, University of Lille I - Ecole des Mines de Douai, France, (1994).

4. **Elmajdoubi, M. and Vu-Khanh, T.**, Theoretical and Applied Fracture Mechanics, 39, N° 2, (2003), 117-126.

5. **Xu, T., Yu, J. and Jin, Z.**, Materials and Design, 22, N° 1, (2001), 27-31.

6. **Karger-Kocsis, J.**, in Polypropylene : Structure, Blends and Composites, 3, Chap 4, J. Karger-Kocsis Ed, Chapman & Hall, London, (1995).

7. **Aurrekoetxea, J., Sarrionandia, M.A., Urrutibeascoa, I. and Maspoch, M.L.I.**, Polymer, 44, N° 22, (2003), 6959-6964.

8. **Dasari, A., Rohrmann, J. and Misra, R.D.K.**, Materials Science and Engineering A, 358, N°1-2, (2003), 372-383.

9. **Varga, J.**, Journal of Materials Science, 27, N° 11, (1992), 2557-2579.

10. **Ourderni, M. and Phillips, P.J.**, Journal of Polymer Science. Part B. Polymer Physics, 33, N° 9, (1995), 1313-1322.

11. **Lafranche, E. and Pabiot, J.**, Journal of Injection Molding Technology, 4, N° 2, (June 2000), 51-64.

12. **Trotignon, J.P. and Verdu, J.**, Journal of Applied Polymer Science, 34, N° 1 (1987) 1-18.

13. **Katti, S.S. and Schultz, J.M.**, Polymer Engineering and Science, 22, N° 16, (1982), 1001-1016.

14. **Kantz, M.R., Newman, H.D. and Stigale, F.H.**, Journal of Applied Polymer Science, 16, N° 5, (1972), 1249-1260.

15. **Varga, J., Breining, A., Ehrenstein, G.W. and Bodor, G.**, International Polymer Processing, 14, N° 4, (1999), 358-364.

16. **Haudin, J.M.**, in Plastic Deformation of Amorphous and Semi-crystalline Materials, B. Escaig & Ch G'Sell Ed., Les Editions de Physique, France, (1982), 292-311

17. **Cermak, R., Obadal, M., Ponizil, P., Polaskova, M., Stoklasa, K. and Lengalova, A.**, European Polymer Journal, 41, N° 8 (2005), 1838-1845.

18. **Cunha, A.M., Pouzada, A.S. and Crowford, R.J.**, Rubber and Composites Processing and Application, 18, N° 2, (1992), 70-90.

19. **Fujiyama, M., Wakino, T. and Kawasaki, Y.**, Journal of Applied Polymer Science, 35, N° 1, (1988), 29-49.

20. **Samuels, R.J.**, *Structured Polymer Properties*, Willey, New York, (1974).

21. **Mavridis, H., Hrymak, A.N. and Vlachopoulos, J.**, Polymer Engineering and Science, 26, N° 7, (1986), 449-455.

22. **Delbarre, P., Pabiot, J., Daurelle, J.F., Lamblin, V. and Rietsch, F.**, *7th* Polymer Processing Society (PPS) Conference, Ontario, Canada, April 24-25, (1991), 282.

23. **Kumaraswamy, G., Verma, R.K., Issaian, A.M., Wang, P., Kornfield, J.A., Yeh, F., Hsiao, B.S. and Olley, R.H.**, Polymer, 41, (2003), 8931-8940.

24. **Karger-Kocsis, J., Mouzakis, D.E., Ehrenstein, G.W. and Varga, J.**, Journal of Applied Polymer Science, 73, (1999), 1205-1214

25. **Van der Wal, A., Mulder, J.J. and Gaymans, R.J.**, Polymer, 39, N° 22, (1998), 5477-5481.

26. **Lafranche, E. and Pabiot, J.**, Journal of Applied Polymer Science, 68, N° 10, (1998), 1661-1669.

27. **Mendoza, R., Regnier, G., Seiler, W. and Lebrun, J.L.**, Polymer, 44, N° 11, (2003), 3363-3373.

28. **Menges, G., Ries, H. and Wiegmann, T.**, Kunststoffe, 77, N° 4, (1987), 433-438.

29. **Fujiyama, M.**, in Polypropylene : Structure,Blends and Composites, 1, Chap 6, J. Karger-Kocsis Ed, Chapman & Hall, London, (1995).

30. **Karger-Kocsis, J. and Benevolenski, O.I.**, Journal of Materials Science, 36, (2001), 3365-3371.